Published in : Polymer (2023), vol. 278, article n°125992
DOI: 10.1016/j.polymer.2023.125992
Status : Postprint (Author's version)

MWCNTs FILLED PCL COVALENT ADAPTABLE NETWORKS: TOWARDS REPROCESSABLE, SELF-HEALING AND FAST ELECTRICALLY-TRIGGERED SHAPE-MEMORY COMPOSITES

Maxime Houbben[a], Clara Pereira Sanchez[b], Philippe Vanderbemden[b], Ludovic Noels[c], Christine Jerome [a],*

[a] *Center for Education and Research on Macromolecules (CERM), University of Liège (ULiège), CESAM-RU, Sart Tilman, Building B6a, B, 4000, Liege, Belgium*
[b] *Department of Electrical Engineering and Computer Science, University of Liège, Liège, Belgium*
[c] *Department of Aerospace and Mechanical Engineering, University of Liège Liège, Belgium*

ABSTRACT

Electrically triggered shape memory polymers efficiency has been proven by numerous studies making them promising novel structural materials for high-end applications. In this field, poly(ε-caprolactone) covalent adaptable networks (PCL-CAN) are particularly appealing since they benefit from excellent shape memory (SM) properties combined with network reconfiguration making easy the design of self-actuated devices of complex shape. Preparation of conducting PCL-CAN networks by melt blending multi-walled carbon nanotubes (MWCNTs) with four-arm star-shaped PCL end-capped with maleimide and furan groups is here investigated. The conventional tensile tester and dynamic mechanical analysis demonstrated the reinforcement of the composite mechanical properties paired with excellent shape memory properties (recovery and fixity ratios about 99%). The simultaneous measurement of the sample resistivity was also integrated to these experiments allowing to follow its evolution during the SM cycles. Rheological measurements highlighted the impact of MWCNTs on the recyclability and self-healing properties of the composite. Electrical triggering of the shape recovery through Joule resistive heating is also deeply studied. The combination of all these properties in the developed material offers unique opportunities to design self-folding multi-materials which is illustrated through the design of smart multi-layered composites. This high-performance composite is especially attractive for reconfiguration of the permanent shape of complex geometry self-deploying devices and their thermal and electrical triggering.

Published in : Polymer (2023), vol. 278, article n°125992
DOI: 10.1016/j.polymer.2023.125992
Status : Postprint (Author's version)

1. Introduction

Shape memory polymers (SMPs) constitute a unique class of materials with remarkable adapting characteristics for a wide range of engineering applications. Covalent networks of semi-crystalline polymers are amongst the most efficient exhibiting high fixity and recovery. Among those, covalent networks of semi-crystalline poly(ε-caprolactone) (PCL) combine remarkable mechanical properties and ease of use thanks to the easily achieved melting temperature (T_m ~ 45 °C).

In the past years, it was demonstrated that introducing in such networks reversible bonds that can reversibly break or connect the chains together imparts the material with additional reprocessing, recycling and reconfiguration abilities [1]. These smart materials find thus advanced applications in various fields, from biomedical microdevices [2-4] to soft robotics and intelligent sensors [5-7]. Among the thermo-reversible bonds used to develop these covalent adaptable networks (CANs), the furan/maleimide Diels-Alder (DA) adduct is well-adapted since it exhibits a fast retro reaction upon moderate heating (~100 °C) [8-11]. So, several shape memory CANs based on this

DA adduct are already reported [12,13]. Some of us previously reported on the synthesis of a furan/maleimide PCL-CAN by melt blending four-arm star-shaped PCL chains end-capped with both reactive groups [14,15] exhibiting the remarkable combination of excellent shape memory properties and reprocessability.

This work aims at imparting this furan/maleimide star-PCL covalent adaptable network (PCL-CAN) with an electrically triggered shape recovery ability thanks to Joule resistive heating. Electric current passing through the material to generate local heating is an easy process to trigger shape recovery avoiding heating of the surrounding area having as advantages of a rapid implementation and remote control. For this purpose, the PCL-CAN has to be filled with a conductive filler. Carbon black nanoparticles, carbon nanofiber, multi-walled carbon nanotubes (MWCNTs) and graphene are commonly used for the preparation of shape memory composites (SMCs) [16]. These fillers improve mechanical, electrical and thermal conductivity of the SMPs from which numerous high-end applications can take benefits. Among them, MWCNTs presents superior electrical and thermal conductivities thanks to low bulk density and high aspect ratio which explains their wide use for SMCs preparation [17].

In this study, the impact of the addition of MWCNTs on the properties of the PCL-CAN composite (PCL-CAN_C) has been investigated by comparing the behavior of PCL-CAN with and without MWCNTs. In depth investigation of the composite properties was made possible by integrating to the conventional characterization methods, namely tensile tester and dynamic mechanical analysis, the simultaneous measurement of the electrical resistivity of the sample. This set-up also allowed the study of the electrical activation of the shape recovery of the system through electromagnetic Joule effect. Rheological measurements demonstrated the recyclability and self-healing ability of this PCL-CAN composite. Finally, taking benefit of the combination of all these properties in the

Published in : Polymer (2023), vol. 278, article n°125992
DOI: 10.1016/j.polymer.2023.125992
Status : Postprint (Author's version)

developed material, the latter was used to construct a smart multi-layered composite device exhibiting self-folding.

2. Materials and methods

2.1. MATERIALS

Multi-walled carbon nanotubes (MWCNTs, Nanocyl) were used as received. 4-arm PCL stars (9000 g/mol) end-capped with furan (PCL_{82}- 4FUR) or maleimide (PCL_{82}-4MAL) were obtained by end-group functionalization of home-made star-shaped PCL-OH according to a previously reported procedure [15,18].

2.2. PREPARATION OF THE PCL COMPOSITE NETWORKS ($PCL\text{-}CAN_C$)

$$Insoluble\ fraction = \frac{dried\ material\ weight}{initial\ material\ weight} \times 100 \quad (1)$$

$$Swelling\ ratio = \frac{(swollen\ gel\ weight - dried\ material\ weight)}{dried\ material\ weight} \times 100 \quad (2)$$

Stoichiometric amounts of end-reactive PCL_{82}-4FUR and PCL_{82}- 4MAL were finely grounded together to produce 4.5 g of blend and then mixed into a vial with 3 wt% of MWCNTs. This mix was then melt-blended for 60 min at 150 rpm and 105 °C in a 6 cm^3 co-rotating twin screw mini-extruder (Xplore, DSM) followed by a rapid injection into a flat sheet mold. For sake of comparison, a PCL-CAN reference sample was prepare following the same procedure without adding the MWCNTs.

2.3. CURING OF THE PCL NETWORKS

The extruded materials were injected in a 0.5 mm-thick squared metallic frame and hot pressed at 105 °C under a load of 4000 kg. Each sample was then placed under a load of 10 kg for 72 h in a ventilated oven at 65 °C. They were recovered in the shape of a flat sheet that was kept for at least 7 days at room temperature before any measurement. This procedure is based on previous studies on furan/maleimide DA shape-memory PCLs [11] and allows the formation of highly crosslinked networks.

2.4. RECYCLING OF $PCL\text{-}CAN_C$

Stripes of the $PCL\text{-}CAN_C$ are cut-up in small parts which are piled in a flat sheet mold and hot pressed at 125 °C for 60 min. The new film is cured at 65 °C for 72 h before being cut-up again and piled for another cycle. This process is repeated up to 3 times and stopped after curing, it delivers a flat recycled PCL-CANc film that has been tested to evaluate its properties after resting a week at room temperature.

Published in : Polymer (2023), vol. 278, article n°125992
DOI: 10.1016/j.polymer.2023.125992
Status : Postprint (Author's version)

2.5. PCL NETWORK SWELLING TEST

About 0.25 g of cross-linked PCL samples collected after curing were weighed (initial material weight) and then submerged into chloroform for 48 h at 25 ° C in order to reach swelling equilibrium. The gel was then carefully collected without the soluble fraction and weighed (swollen network weight). The gel is then dried under vacuum of 5 x 10^{-2} mmHg at room temperature (~25 °C) until reaching constant weight which is then measured (dried network weight). The insoluble fraction (i.e. network fraction, without the soluble fraction due to unreacted chains or monomers) and the swelling ratio were calculated based on equations (1) and (2) respectively.

2.6. CHARACTERIZATION TECHNIQUES

Differential scanning calorimetry (DSC) analyses were carried out with a TA DSC 250 apparatus. Endotherm and melting point were determined during the second heating run between -80 °C and 100 °C at 10 °C/min with 5 min isotherms at each end-cycle temperatures. The degree of crystallinity has been evaluated by comparing the measured melting enthalpy to the one reported for a 100% crystalline PCL.

Shape-memory properties have been measured by dynamic mechanical analysis (DMA) on a TA Q800 in controlled force mode with a tensile clamp. The sample (15 mm x 5 mm x 0.5 mm) was first equilibrated at 65 °C for 5 min then experienced a tensile stress ramp (0.06 MPa/min) till 0.6 MPa. Then, the sample is cooled down, under stress at 3 °C/min to 0 °C and maintained at that temperature for 5 min. The stress is then released and the sample is reheated, stress-free at 3 °C/min to 65 °C. The process is here cycled 4 times. The strain comparison at 0 °C before and after stress release allows the measurement of the sample fixity. The fixity ratio (R_f) is given by equation (3). The shape recovery ratio is measured by strain comparison at 65 °C before and after cycling, the recovery ratio (R_c) being calculated by equation (4).

$$R_f = \frac{strain\ after\ stress\ release\ at\ 0°C}{strain\ before\ stress\ release\ at\ 0°C} * 100 \quad (3)$$

$$R_c = \frac{strain\ at\ 65°C\ without\ stress\ for\ cycle\ N\ at\ 0°C}{strain\ at\ 65°C\ without\ stress\ for\ cycle\ N-1} * 100 \quad (4)$$

Electrical resistivity measurements were performed on rectangular samples (15 mm x 5 mm x 0,5 mm) cleaned in isopropanol and painted on their surface with silver paste (Agar scientific Electrodag 1415) following a previously described four-point method [19]. Thin copper wires were used to inject the current through their length. A Keithley 2400 source controlled by LabVIEW program was used to inject the current set to the lowest possible value (0.5 mA), at which no measurable resistive heating occurs. A Keithley 2001 multimeter was used to measure the voltage.

During self-heating experiments, the sample is vertically suspended by taking advantage of the copper wires. The front surface temperature of the sample is measured using an infrared thermal camera (COX CX320) that was previously in-house calibrated [19]. To achieve a well-defined resistive heating and temperature ramp, the value of the injected current is set by a proportional integral

Published in : Polymer (2023), vol. 278, article n°125992
DOI: 10.1016/j.polymer.2023.125992
Status : Postprint (Author's version)

controller allowing to adjust the value of the injected current (up to 0,013 A) as previously described by our group [19].

Rheological measurements were performed on an ARES-G2 Rheometer from TA Instruments. 1 g of a sample disk was placed at 125 ˚C in a plate-plate geometry (diameter 25 mm). The temperature was then decreased and adjusted to the various studied values where both the elastic and viscous moduli were recorded through time at a frequency of 1Hz and a strain of 1%.

3. Results and discussion

3.1. PCL COMPOSITE NETWORK PREPARATION

As previously reported [14,15], PCL covalent adaptable networks (PCL-CAN) can be prepared by melt blending a mixture of 4-arm PCL stars bearing maleimide or furan moieties at the chain-ends in a stoichiometric amount. By controlling the temperature, a thermo-reversible PCL-CAN is obtained by the formation of Diels-Alder adducts below 125 °C between both types of stars (Fig. 1). This network can be cleaved back to a fluid mixture of the stars by heating above 125 °C. In the polymer stability range (below 150 °C), the blending of the PCL_{82}-4MAL with PCL_{82}-4FUR will lead to a reversible network (PCL-CAN). With the goal to impart conductivity to this PCL-CAN network, 3 wt% of MWCNTs were added to the blend. As evidenced in a previous paper [19], using 1 wt% of MWCNTs leads to an average resistivity of the composite below 80 Ω.m, i.e., low enough to enable current driven heating. Nevertheless, 3 wt% of MWCNTs insures a better reproducibility of the resistive heating especially upon high deformation of the material, while preserving a good dispersion of the filler in the matrix.

Since it is reported that Diels-Alder reaction can occur between MWCNTs and furan or maleimide moieties, we investigated first the impact of the MWCNTs addition on the network formation. A first evidence of the occurrence of some PCL stars grafting on the MWCNTs during melt-blending at 105 °C is the small torque increase observed while processing for 1 h the PCL stars which is not the case in absence of MWCNTs.

After appropriate curing, the network formation has been compared for the PCL-CAN with and without MWCNTs by swelling tests in $CHCl_3$ a good solvent for the PCL stars. The same very high insoluble fraction is observed for both samples (Table 1). This shows the large extend of reaction of the stars. The presence of the MWCNTs in the PCL network decreases the swelling in $CHCl_3$.

Studying several reports in literature, the impact of carbon nanotubes on the polymer matrix crystallization is shown dependent on the nature of the polymer matrix, the degree of dispersion, the CNT-polymer interactions, the thermal treatment, or other parameters, but also from study to study [20-28]. Generally, it is shown that MWCNTs can act as efficient nucleation agents, thus increasing the rate of polymer crystallization, which influences the crystallization temperature, the degree of crystallinity and crystallite sizes [29,30]. Here, the overall degree of crystallinity of PCL-CAN_c is slightly superior compared to the network without fillers (Table 1) and the melting still occurs at 43 °C. A faster crystallization close to room temperature is however observed for the composite

Published in : Polymer (2023), vol. 278, article n°125992
DOI: 10.1016/j.polymer.2023.125992
Status : Postprint (Author's version)

which would facilitate the fixing of the temporary shape upon cooling. The melting temperature remaining slightly above the body temperature, this shape memory composite preserves the appealing property of a shape recovery to be externally triggered without need of overheating that could damage the surrounding tissues, opening perspectives for biomedical applications.

3.2. SHAPE MEMORY PROPERTIES AND ELECTRICAL BEHAVIOR

The shape-memory performances have been compared for the networks with (PCL-CAN$_C$) and without (PCL-CAN) MWCNTs. Fig. 2. I shows the detailed DMA curve recorded for 4 successive shape-memory cycles for PCL-CAN$_C$ and Fig. 2. II for PCL-CAN. During the stress- controlled elongation of at 65 °C (A to B), an almost linear deformation is observed for both PCL networks. From the slope, the obtained Young modulus is 0.032 N/m^2 for PCL-CAN$_C$ and 0.018 N/m^2 for PCL- CAN showing the reinforcement effect of the MWCNTs in the composite network. Upon cooling, both profiles are similar. Oriented crystallization occurs and is responsible of a further increase of the elongation at constant stress [31] (B to C), as previously observed for similar PCL-CAN [32,33]. A very high fixity (R_f above 99%, Table 2) is obtained for each cycle and both samples thanks to the PCL crystallinity which is typical for shape-memory materials based on crystallization as the fixing process, especially when the degree of crystallization is high, such as for PCL. The shape recovery is then triggered by a temperature above 45 °C (D to A). Classically, a training phenomenon is observed after the first cycle which thus shows the lowest recovery, while the following cycles are all characterized by excellent shape recovery ratios, i.e., higher than 96% (Table 2).

As already reported [31], in the case of furan-maleimide CAN, a steady increase of the strain is observed from cycle to cycle. This phenomenon is attributed to the occurrence of retro-DA reactions upon tensile stress. Some DA adducts then undergoing cycloreversion, it leads to the relaxation of the debonded polymer chains, pulling apart the chain-ends, that will not couple back during the cycle. This phenomenon occurs at each cycle, leading to a repetitively slight decrease of the crosslink density resulting in a more ductile material. This phenomenon is less pronounced for PCL-CAN$_c$ thanks to the reinforcement of the MWCNTs which support part of the stress leading to a reduced elongation of the network. Thus, the presence of the MWCNTs preserves the high SM properties of the CAN, reinforces the network increasing the modulus at high temperature and reduces the stress induced debonding from cycle to cycle improving repeatability.

In case of PCL-CAN$_C$, the shape recovery can be triggered by the Joule effect. With 3 wt% of MWCNTs concentration, the composite is well above the percolation threshold. The measured electrical resistivity (ρ_e) is 0.075 ± 0.025 Ω.m at 20 °C without load. Using a home-made set-up integrating the measurement of the electrical resistivity in the DMA equipment, the variation of the resistivity during the shape memory cycles could be monitored. Fig. 2. III shows the evolution of the electrical resistivity (relatively to its value at the beginning of the experiment) simultaneously to the DMA experiment. It evidences that ρ_e varies during a SM cycle with a maximum increase of a factor 2, ρ_e reaching 0.15 ± 0.025 Q.m at its maximum. The minimum resistivity is observed at high temperature when the PCL is in the molten state and when the system has the most mobility facilitating the contacts between the nanotubes and thus charge tunnelling. At low temperature, when the PCL is crystallized, the reduced mobility of the system and frozen crystalline areas lead to the rupture of

Published in : Polymer (2023), vol. 278, article n°125992
DOI: 10.1016/j.polymer.2023.125992
Status : Postprint (Author's version)

some conducting paths leading to an increase of the resistivity by a factor 1.5. In addition, this experiment also reveals that the resistivity goes through a maximum during the phase transition of the PCL whatever the transition, melting or crystallization. As a consequence, a resistivity drop of a factor 2 is occurring and should be eventually considered when performing electrically- triggered shape-recovery. Even though, the SMCs remain conductive enough to allow a Joule effect and efficient heating of stretched samples and to insure reproducibility between experiments.

As shown in Fig. 3., PCL-CAN_C allows a well-controlled, homogeneous and fast heating of the sample by Joule effect. A linear heating ramp from room temperature to 60 °C with a rate of 10 °C/min can be obtained by controlling the injected electric current passing through the composite network. A linear cooling ramp from 60 °C to the room temperature is achieved with a similar rate by progressively decreasing the current. As evidenced by the temperature recorded at different locations (Fig. 3 - P2 to P6) of the PCL-CAN_C stripe, the sample is heating uniformly by the injected electrical current.

Such a heating ramp was thus applied to a PCL- CAN_C network fixed in a temporary shape in order to trigger the shape recovery (Fig. 4). The rectangular sample (41.2 mm x 8.1 mm x 0.5 mm) initially stretched in the temporary shape (length stretched sample 62.87 mm) recovers its original shape in 2 min by injecting increasing current from room temperature (25 °C). Interestingly, it was observed that the sample heats up faster in stretched areas as illustrated by the pictures of the thermal camera (Fig. 4) showing that the undeformed area close to the grip remains underheated. This advantageously allows triggering the shape recovery without overheating the entire sample above 45 °C.

3.3. RECYCLING

Thanks to the furan-maleimide adduct that undergoes significant cyclo-reversion at temperature above 100 °C [34], PCL-CAN can be recycled at high temperature. Rheological measurements were performed to study the impact of the MWCNTs addition on the PCL-CAN network reversibility. Three heating/cooling cycles were performed at the two optimal temperatures, i.e., 65 °C for DA adduct formation and 125 °C for retro DA reaction. Staying above the melting temperature of the PCL (> 45 °C) during the experiment confers enough mobility to the polymer chains enabling crosslinking by the creation of the DA adduct but it also prevents perturbations due to PCL crystallites during the rheological measurement. Fig. 5 compares the evolution of the storage and loss moduli during these thermal cycles for PCL-CAN and PCL-CAN_C.

Before starting the experiment, the samples are equilibrated for 1 h at 125 °C in the rheometer (not recorded) to shift the equilibrium towards the retro-DA reaction. In both cases, the network breaks up since at the start of the analysis, a viscous behavior is observed, the loss modulus (G'') dominating the storage modulus (G'). Even in presence of the MWCNTs, the CAN goes back to viscous liquid upon retro-DA reaction. The temperature is then decreased until 65 °C leading to an increase of both moduli.

Published in : Polymer (2023), vol. 278, article n°125992
DOI: 10.1016/j.polymer.2023.125992
Status : Postprint (Author's version)

Both moduli continuously increase during the isotherms at 65 ˚C, which can be attributed to the progressive network formation since G' and G'' remain constant for PCL_{82}-4OH at 65 °C. After 120 min, the moduli were still increasing meaning that the DA equilibrium is not achieved yet under these conditions, nevertheless the isotherm is stopped and the temperature is increased back to 125 °C to shift again the equilibrium towards retro-DA and to test the reversibility. A 1-h isotherm turned out to be more than sufficient to reach the thermodynamic equilibrium and an uncrosslinked state since the G' and G" reach a plateau for all isotherms. The faster kinetics of the retro-DA reaction, compared to the DA reaction is explained by the fast disruption of the DA adduct which is a monomolecular reaction compared to the DA addition that is bimolecular and where an efficient coupling of furan and maleimide chain-ends in the PCL bulk is mandatory. Furthermore, in case of the DA reaction, the diffusion rate is continuously decreased due to the network formation, which slows down the bimolecular coupling of both reactive moieties. Repeated cycling shows similar profiles confirming the remarkable network reversibility even if in case of the composite, the storage modulus at 125 °C tends to increase with the number of cycles. This behavior originates from the progressive irreversible grafting of PCL-fur and PCL-mal on the surface of the MWCNT [35]. Indeed, this increase of G' at 125 °C upon repeated cycling is not observed for non-reactive PCL-OH stars.

In addition, except at the start of the experiment, G' is dominating G'' in the case of the PCL-CAN composite. This is accounted by the formation of a polymer/nanotubes network through the polymer chain/ MWCNT/polymer chain bridging inducing a significant alteration of the viscoelastic terminal zone when above the percolation threshold [36-40]. At low frequency, G' of PCL-CAN_c prevails over G'' marking a clear difference with respect to the polymer melts (PCL-CAN, Figs. 8 and 125 °C) and non-percolated dispersions [39]. The same observation is made on PCL_{82}-4OH with a content of 3 wt% MWCNTs. This result confirms the existence of a percolated network in PCL-CAN_C in accordance to TEM analysis.

Significant reversibility of the PCL-CANc crosslinks being evidenced by rheology, the reprocessability of these composites was considered. Cut-up parts of PCL stripes were piled in a flat sheet mold and hot pressed into another sample as described in Fig. 6I.

Similar swelling ratios and insoluble fractions were obtained for either the sample recycled once or three times as show in Table 3 which suggests that the SMCs are crosslinked in similar extent. Shape memory cycling was conducted on both PCL-CAN_C and PCL-CAN_C recycled networks and their shape memory properties are displayed in Tables 2 and 4 respectively. Both samples exhibit excellent fixity (>99%) and recovery (> 96%) for cycle 2, 3 and 4. When comparing the three curves, the main arising difference is the higher strain experienced by the recycled networks (1 time and 3 times) for the same applied stress. It again reflects the decrease of the degree of crosslinking of the PCL network due to the reaction of furan and maleimide with the MWCNTs surface, phenomena that is enhanced with recycling. Nevertheless, the general behaviour of recycled material does not vary from the original one, i.e., the steady increase in strain from cycle to cycle is also present and can be related too to the same occurrence of retro-DA reactions upon tensile stress.

Interestingly, if recycling is conducted over a smaller time scale, i.e., hot pressing for 15 min at 125 °C, the mechanical performances of the recycled SMCs are similar to the one presented in Fig. 6. II.

Published in : Polymer (2023), vol. 278, article n°125992
DOI: 10.1016/j.polymer.2023.125992
Status : Postprint (Author's version)

Reducing the curing time at 125 °C appears to limit the side-reaction of the furan/ maleimide with the MWCNT.

3.4. SELF-HEALING

Considering the reversibility of the maleimide-furan network, selfhealing was studied by two different thermal repairing processes: convection heating and electrical heating. In both cases, the shape memory effect plays an important assistance to the self-healing process. When external force damages the material up to fracture, the break in the continuity of the matrix is subjected to mechanical deformation which prevents high contact between the crack borders (Fig. 7B). Initial morphology of the fracture is however quickly recovered at high temperature thanks to the shape memory effect which brings back in close contact the crack borders and consequently fasten the healing process and its efficiency (Fig. 7C) [41]. SEM was used to characterize the morphology of the cracked surfaces and healed samples for PCL-CAN_C with convection heating Fig. 7. II) and PCL-CAN_C with resistive heating (Fig. 7. III).

The material was prepared so that its surface was flat and smooth (Fig. 7A). A scratch was made on the sample surface by knife-cutting (Fig. 7B). The damaged sample was then thermally treated at 90 °C for 20 min (Fig. 7C). Then, thermal healing was conducted in a ventilated oven at constant temperature. The fracture was immediately narrowed by shape recovery when T_m is reached and the two cut sections are then in full contact. Partial debonding of the DA adduct is carried during this thermal treatment which makes the two new exposed PCLs border adhesive to one another. The cross-linked networks are then reformed during a second curing treatment at 65 °C for 3 days in a ventilated oven, leading to self-repair (Fig. 7D). The crack-healing ability of the developed materials is thus demonstrated.

When repaired either by convection or electric heating, the narrowing crack shape memory effect of the PCL-CAN_C is quickly triggered within 1 min of heating. The main particularity of internal self-heating by Joule effect is the local increase of the temperature in the damaged area due to the local increase of resistivity at the tip of the cracks [42]. Results demonstrated high-efficiency and repeatability of the PCL-CAN_C self-healing performance via both electrical and thermal healings indicating the high potential for various uses in industrial applications. As the DA reaction occurs even at room temperature, the thermal treatment imposed to the samples after the crack narrowing could be avoided and the sample would simply self-heal over a longer time period. Simple implementation of cracks detection through temperature monitoring or crack growth arrest through self-healing leads to the preparation of smart and low energy cost self-healing materials.

3.5. MULTI-LAYERED ELECTRO-ACTIVE SMART SMC

The developed PCL-CAN_C exhibiting auto-repair abilities offers straightforward processing perspectives to design multilayer devices of complex shapes such as self-deploying devices with sequential triggering of the shape recovery. Covalent crosslinking between several layers of PCL-CAN/PCL-CAN_C can easily be implemented to assemble a multi- SMP/SMC layers composite. This is

Published in : Polymer (2023), vol. 278, article n°125992
DOI: 10.1016/j.polymer.2023.125992
Status : Postprint (Author's version)

here illustrated through the preparations of a smart multi-layered composite presenting a sequential shape memory behavior as demonstrated in Fig. 8. CAN systems can simply be juxtaposed (Fig. 8. I) next to each other in a specific configuration and heated up for uncrosslinking before being crosslinked back into a single piece (Fig. 8. II). The sandwich-like structure is composed of layers either conductive (PCL-CAN$_C$) or not (PCL-CAN) that can be arranged in different patterns (Fig. 8. III). Once the smart SMC is designed, it can be easily programmed in a temporary shape and then by triggering shape recovery selectively in one layer, a transition to a second temporary shape occurs by self-folding of the device (Fig. 8. IV). In the present example, the bilayer sample self-folds into a L-bended shape. Finally, by maintaining the current ramp in the active layer for an extended period of time, conduction heat from the conductive layer heats up the insulating layer (PCL-CAN) and triggers the return of the device to the permanent shape. The fine control of the current through the device allows thus the progressive transformation in various programmed shapes thanks to dedicated design of the smart multi-layered of PCL- CAN and its MWCNT composites.

Figure 1. *Sketch of the progressive network formation in function of the Maleimide- Furan Diels-Alder addition.*

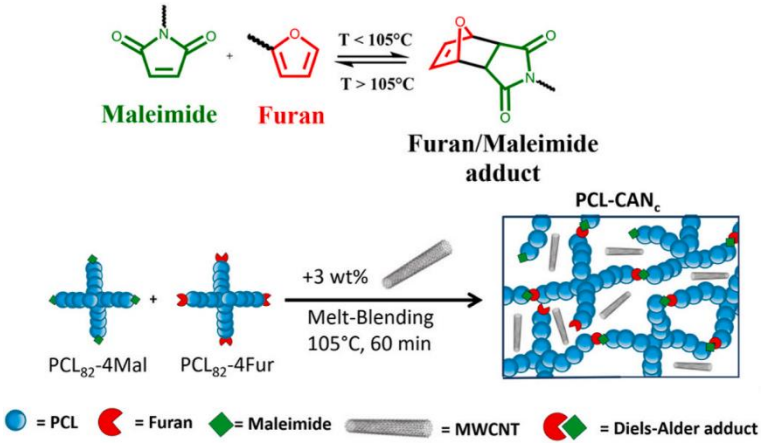

Table 1. *Swelling ratio, insoluble fraction, crystallinity, T_m and T_c of the PCL-CAN and PCL-CAN$_C$ networks.*

	PCL-CAN	PCL-CAN$_C$
Swelling ratio (%)	925	682
Insoluble fraction (%)	98,5	98,5
Crystallinity degree (%)	32,8	34,6
T_m (C°)	43,1	43,3
T_c (C°)	16,7	26,6

Published in : Polymer (2023), vol. 278, article n°125992
DOI: 10.1016/j.polymer.2023.125992
Status : Postprint (Author's version)

Figure 2.

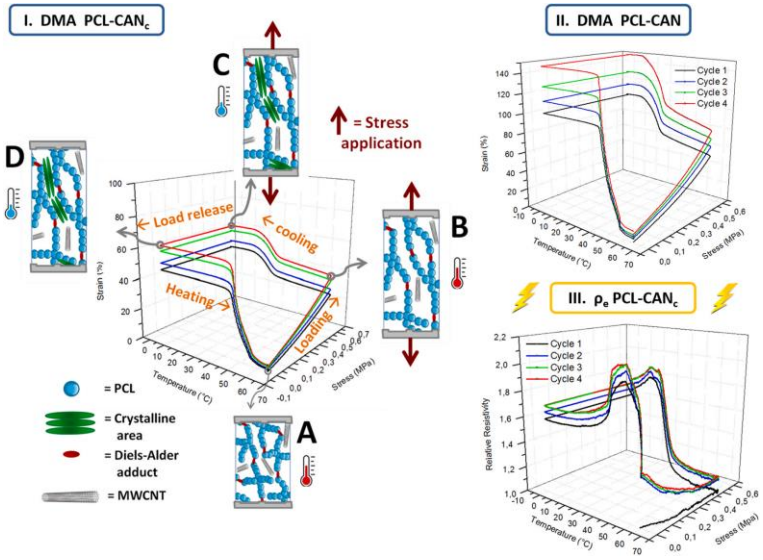

Shape-memory cycles evaluated by DMA upon convection heating/cooling of PCL-CAN (II) and PCL-CAN$_C$(I) networks after 14 days at room temperature, III. Monitoring of the relative electrical resistivity in a PCL-CAN$_C$ network concomitantly to its respective shape memory cycle (Fig. 5 - I).

Table 2. *Shape memory properties of PCL-CAN and PCL-CAN$_C$ networks.*

PCL-CAN				
	Cycle 1	*Cycle 2*	*Cycle 3*	*Cycle 4*
Fixity Ratio, Rf (%)	99,47	99,99	99,99	99,99
Recovery Ratio, Rc (%)	95,43	98,25	98,53	97,43
Maximal Strain (%)	101,48	113,65	128,06	147,71
PCL-CAN$_C$				
	Cycle 1	*Cycle 2*	*Cycle 3*	*Cycle 4*
Fixity Ratio, Rf (%)	99,44	99,52	99,54	99,56
Recovery Ratio, Rc (%)	96,38	98,52	97,69	96,13
Maximal Strain (%)	44,16	48,75	52,71	56,56

Published in : Polymer (2023), vol. 278, article n°125992
DOI: 10.1016/j.polymer.2023.125992
Status : Postprint (Author's version)

Figure 3. *Controlled heating (I) and cooling (II) ramps of PCL-CANC by Joule effect with a rate of 10 °C·min- and infrared images of both heating (III) and cooling (IV) PCL-CANC samples.*

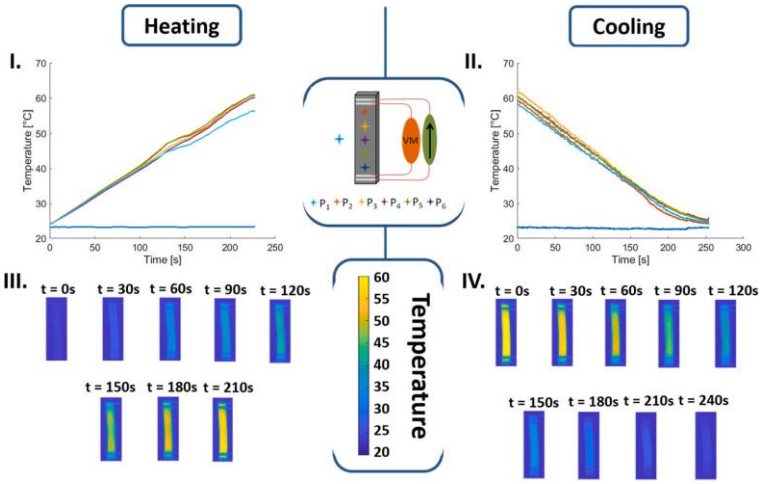

Figure 4. *Classical and infrared images of electro-active shape memory recovery process by electrically controlled Joule effect.*

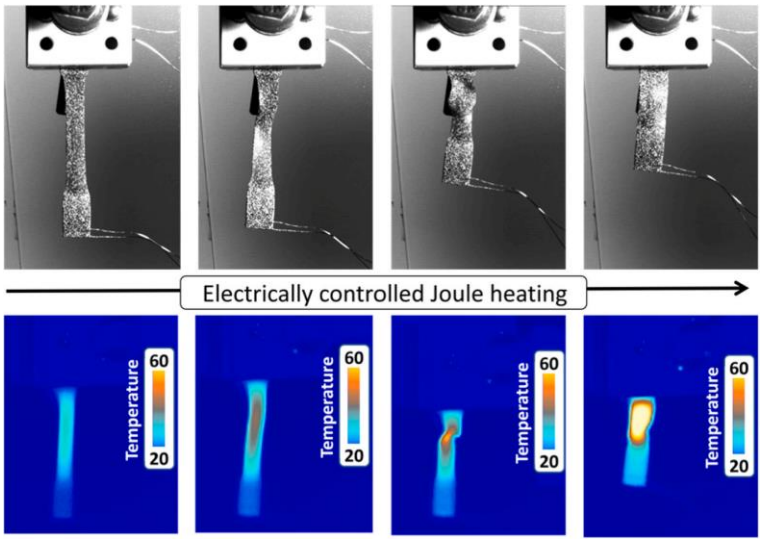

Figure 5. *Rheometer study of thermoreversibility of crosslinking of PCL-CAN and PCL-CAN$_C$ with isotherm time of respectively 1 h at 125 °C and 2 h at 65 °C.*

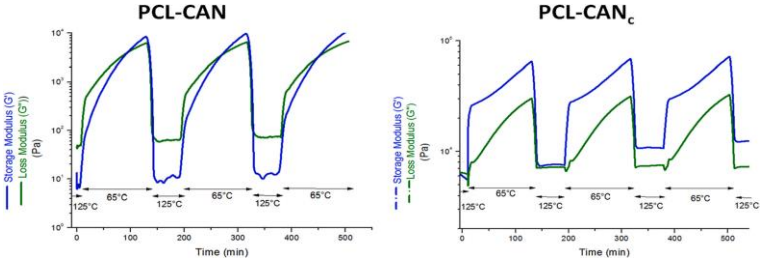

Published in : Polymer (2023), vol. 278, article n°125992
DOI: 10.1016/j.polymer.2023.125992
Status : Postprint (Author's version)

Table 3. *Swelling ratio and insoluble fraction of the PCL-CAN$_C$ recycled network.*

Recycling cycles	Swelling ratio	% insoluble
0 x (Original)	682	98,50
1 x	1012,24	92,45
3 x	1047,06	91,69

Table 4. *Shape memory properties PCL-CAN$_C$ recycled networks.*

PCL-CAN$_C$ - Recycled 1 time				
	Cycle 1	*Cycle 2*	*Cycle 3*	*Cycle 4*
Fixity Ratio, R_f(%)	99,47	99,99	99,99	99,99
Recovery Ratio, R_c (%)	87,07	97,89	96,15	98,35
Maximal Strain (%)	70,75	78,24	86,59	94,25
PCL-CAN$_C$ - Recycled 3 times				
	Cycle 1	*Cycle 2*	*Cycle 3*	*Cycle 4*
Fixity Ratio, R_f(%)	99,70	99,73	99,73	99,74
Recovery Ratio, R_c (%)	90,50	96,82	97,04	99,16
Maximal Strain (%)	99,77	114,27	127,30	153,83

Figure 6. *Rheometer study of thermoreversibility of crosslinking of PCL-CAN and PCL-CAN$_C$ with isotherm time of respectively 1 h at 125 °C*

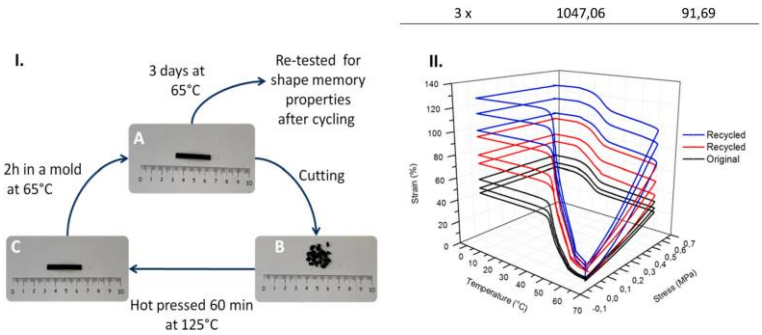

I - Demonstration of PCL-CAN$_C$ recyclability. Stripes of the SMP$_C$ (A) are cut-up in small parts (B) which are piled in a flat sheet mold and hot pressed at 125 °C for 60 min. The new film is cooled down to 65 °C for 2 h before being cut-up again and piled for another cycle. This process is repeated 3 times and delivers a flat PCL- CAN$_C$ film (C). This film is cured for 72 h at 65 °C to form again an SMP$_C$ that has been tested to evaluate its properties; II - Shape-memory properties evaluated by thermo-mechanical cycling of the recycled PCL-CAN$_C$ networks measured 7 days after end of curing.

Published in : Polymer (2023), vol. 278, article n°125992
DOI: 10.1016/j.polymer.2023.125992
Status : Postprint (Author's version)

Figure 7.

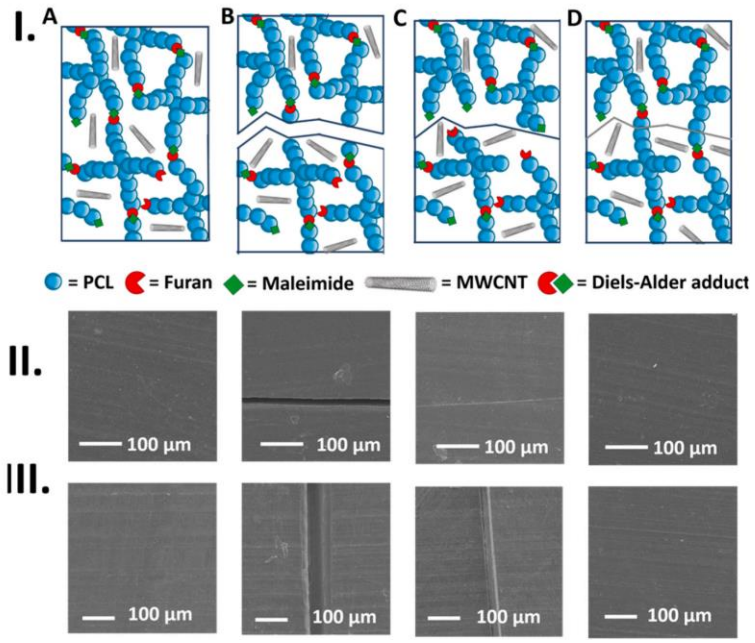

Schematic illustration of the self-healing process (I), convection self-healing (II), electrical self-healing (III) of a PCL-CAN$_C$: initial material (A), cracked material (B), reduction of the crack gap by thermal triggered shape memory effect (C - 90 °C, 20 min), healed material by formation of new covalent bonds (D - 65 °C, 3 days).

Figure 8. *Preparation by hot molding and activation of smart multi-layered SMC by Joule heating.*

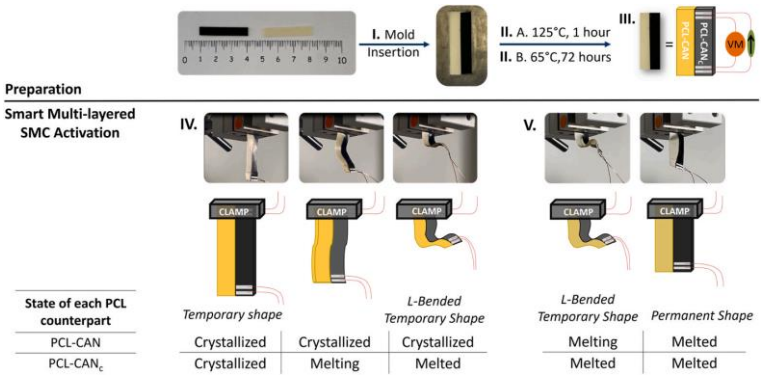

4. Conclusions

In this work, a smart shape memory self-healable and recyclable composite was developed from PCL covalent adaptable networks. In-depth investigation of the Joule effect triggered shape memory properties was made possible by integrating to the conventional characterization methods, namely tensile tester and dynamic mechanical analysis, the simultaneous measurement of the sample resistivity. The electrical activation of the shape recovery through Joule effect is particularly attractive to finely control the triggering of the shape recovery while avoiding overheating of the surrounding. This is especially of interest when a sequential recovery of a multi-material device is

Published in : Polymer (2023), vol. 278, article n°125992
DOI: 10.1016/j.polymer.2023.125992
Status : Postprint (Author's version)

foreseen. Indeed, it allows to trigger shape transitions in dedicated parts of multilayered materials allowing the precise control of multiple and progressive shape transitions. In addition, this easy to reprocess and reconfigurable PCL-CAN material makes straightforward the elaboration of multilayered smart devices of various conductivities by loading or not the network with MWCNTs allowing fabrication of self-deploying devices of complex shapes integrating parts with selectively triggered shape recovery.

CREDIT AUTHORSHIP CONTRIBUTION STATEMENT

MAXIME HOUBBEN: Investigation, Data curation, Writing - original draft, Visualization. CLARA PEREIRA SANCHEZ: Investigation, Resources. PHILIPPE VANDERBEMDEN: Conceptualization, Methodology, Validation, Formal analysis, Writing - review & editing, Funding acquisition, Resources. LUDOVIC NOELS: Conceptualization, Writing - review & editing, Project administration, Funding acquisition, Resources. CHRISTINE JÉRÔME: Conceptualization, Methodology, Validation, Formal analysis, Writing - review & editing, Supervision, Project administration, Funding acquisition, Resources.

DECLARATION OF COMPETING INTEREST

The authors declare that they have no known competing financial

interests or personal relationships that could have appeared to influence the work reported in this paper.

DATA AVAILABILITY

Data will be made available on request.

ACKNOWLEDGEMENT

This research was funded through the "Actions de recherche concertées 2017 - Synthesis, Characterization, and Multiscale Model of Smart Composite Materials (S3CM3) 17/21-07", financed by the "Direction Générale de l'Enseignement non obligatoire de la Recherche scientifique, Direction de la Recherche scientifique, Communauté française de Belgique et octroyées par l'Académie Universitaire Wallonie- Europe"

Published in : Polymer (2023), vol. 278, article n°125992
DOI: 10.1016/j.polymer.2023.125992
Status : Postprint (Author's version)

References

1) W. Zou, J. Dong, Y. Luo, Q. Zhao, T. Xie, Dynamic covalent polymer networks: from old chemistry to modern day innovations, Adv. Mater. 29 (2017), https://doi. org/10.1002/adma.201606100.

2) W. Yan, Y. Ding, R. Zhang, X. Luo, P. Sheng, P. Xue, J. He, Dual-functional polymer blends with rapid thermo-responsive shape memory and repeatable self-healing properties, Polymer 239 (2022), 124436, https://doi.org/10.1016/j.polymer.2021.124436.

3) Y. Chen, X. Zhao, C. Luo, Y. Shao, M.-B. Yang, B. Yin, A facile fabrication of shape memory polymer nanocomposites with fast light-response and self-healing performance, Composites Part A Appl Sci Manuf 135 (2020), 105931, https://doi. org/10.1016/j.compositesa.2020.105931.

4) H. Pandey, S.S. Mohol, R. Kandi, 4D printing of tracheal scaffold using shapememory polymer composite, Mater. Lett. (2022), 133238, https://doi.org/ 10.1016/j.matlet.2022.133238.

5) X. Wang, J. Lan, P. Wu, J. Zhang, Liquid metal based electrical driven shape memory polymers, Polymer 212 (2021), 123174, https://doi.org/10.1016Zj. polymer.2020.123174.

6) Romo-Uribe, Robust POSS-PEG networks. Nanostructure, viscoelasticity and shape memory behavior, Polymer 250 (2022), 124899, https://doi.org/10.10167j. polymer.2022.124899.

7) M. Song, X. Liu, H. Yue, S. Li, J. Guo, 4D printing of PLA/PCL-based biopolyurethane via moderate cross-linking to adjust the microphase separation, Polymer 256 (2022), 125190, https://doi.org/10.1016/j.polymer.2022.125190.

8) Z. Li, R. Yu, B. Guo, Shape-memory and self-healing polymers based on dynamic covalent bonds and dynamic noncovalent interactions: synthesis, mechanism, and application, ACS Appl. Bio Mater. 4 (2021) 5926-5943, https://doi.org/10.1021/ acsabm.1c00606.

9) H. Bi, G. Ye, H. Sun, Z. Ren, T. Gu, M. Xu, Mechanically robust, shape memory, selfhealing and 3D printable thermoreversible cross-linked polymer composites toward conductive and biomimetic skin devices applications, Addit. Manuf. 49 (2022), 102487, https://doi.org/10.1016/j.addma.2021.102487.

10) J. Caprasse, R. Riva, J.-M. Thomassin, C. Jerome, Hybrid covalent adaptable networks from cross-reactive poly(e-caprolactone) and poly(ethylene oxide) stars towards advanced shape-memory materials, Mater Adv 2 (2021) 7077-7087, https://doi.org/10.1039/D1MA00595B.

11) H. Ouyang, X. Li, X. Lu, H. Xia, Selective laser sintering 4D printing of dynamic cross-linked polyurethane containing diels-alder bonds, ACS Appl Polym Mater 4 (2022) 4035-4046, https://doi.org/10.1021/acsapm.2c00565.

12) G. Rivero, L.T.T. Nguyen, X.K.D. Hillewaere, F.E. du Prez, One-pot thermo- remendable shape memory polyurethanes, Macromolecules 47 (2014) 2010-2018, https://doi.org/10.1021/ma402471c.

13) M.D. Hager, S. Bode, C. Weber, U.S. Schubert, Shape memory polymers: past, present and future developments, Prog. Polym. Sci. 49-50 (2015) 3-33, https:// doi.org/10.1016/j.progpolymsci.2015.04.002.

14) T. Defize, J.-M. Thomassin, M. Alexandre, B. Gilbert, R. Riva, C. Jerome, Comprehensive study of the thermo-reversibility of Diels-Alder based PCL polymer networks, Polymer 84 (2016) 234-242, https://doi.org/10.1016/j.polymer.2015.11.055.

Published in : Polymer (2023), vol. 278, article n°125992
DOI: 10.1016/j.polymer.2023.125992
Status : Postprint (Author's version)

15) M. Houbben, J.-M. Thomassin, C. Jérôme, Supercritical CO2 blown poly (e-caprolactone) covalent adaptable networks towards unprecedented low density shape memory foams, Mater Adv 3 (2022) 2918-2926, https://doi.org/10.1039/ D2MA00040G.

16) T. Khan, M.S. Irfan, M. Ali, Y. Dong, S. Ramakrishna, R. Umer, Insights to low electrical percolation thresholds of carbon-based polypropylene nanocomposites, Carbon N Y 176 (2021) 602-631, https://doi.org/10.1016/j.carbon.2021.01.158.

17) E. Tekay, Preparation and characterization of electro-active shape memory PCL/ SEBS-g-MA/MWCNT nanocomposites, Polymer 209 (2020), 122989, https://doi. org/10.1016/j.polymer.2020.122989.

18) W.H. Heath, F. Palmieri, J.R. Adams, B.K. Long, J. Chute, T.W. Holcombe, S. Zieren, M.J. Truitt, J.L. White, C.G. Willson, Degradable cross-linkers and strippable imaging materials for step-and-flash imprint lithography, Macromolecules 41 (2008) 719-726, https://doi.org/10.1021/ma702291k.

19) C. Pereira Sanchez, M. Houbben, J.-F. Fagnard, P. Harmeling, C. Jerome, L. Noels, P. Vanderbemden, Experimental characterization of the thermo-electro-mechanical properties of a shape memory composite during electric activation, Smart Mater. Struct. 31 (2022), 095029, https://doi.org/10.1088/1361-665X/ac8297.

20) Göldel, A. Marmur, G.R. Kasaliwal, P. Pötschke, G. Heinrich, Shape-dependent localization of carbon nanotubes and carbon black in an immiscible polymer blend during melt mixing, Macromolecules 44 (2011) 6094-6102, https://doi.org/ 10.1021/ma200793a.

21) Toda, R. Androsch, C. Schick, Insights into polymer crystallization and melting from fast scanning chip calorimetry, Polymer 91 (2016) 239-263, https://doi.org/ 10.1016/j.polymer.2016.03.038.

22) Y.F. Chen, Y.J. Tan, J. Li, Y.B. Hao, Y.D. Shi, M. Wang, Graphene oxide-assisted dispersion of multi-walled carbon nanotubes in biodegradable Poly (e-caprolactone) for mechanical and electrically conductive enhancement, Polym. Test. 65 (2018) 387-397, https://doi.org/10.1016/j.polymertesting.2017.12.019.

23) X. Xu, P. Fan, J. Ren, Y. Cheng, J. Ren, J. Zhao, R. Song, Self-healing thermoplastic polyurethane (TPU)/polycaprolactone (PCL)/multi-wall carbon nanotubes (MWCNTs) blend as shape-memory composites, Compos. Sci. Technol. 168 (2018) 255-262, https://doi.org/10.1016/j.compscitech.2018.10.003.

24) Huang, C. Vyas, I. Roberts, Q.A. Poutrel, W.H. Chiang, J.J. Blaker, Z. Huang, P. Bartolo, Fabrication and characterisation of 3D printed MWCNT composite porous scaffolds for bone regeneration, Mater. Sci. Eng. C 98 (2019) 266-278, https://doi.org/10.1016/j.msec.2018.12.100.

25) A.M. El Sayed, Synthesis, optical, thermal, electric properties and impedance spectroscopy studies on P(VC-MMA) of optimized thickness and reinforced with MWCNTs, Results Phys. 17 (2020), 103025, https://doi.org/10.1016/j. rinp.2020.103025.

26) V. Lorenzelli, Advances in Polymer Science, vol. 54, Spectroscopy, 1984, https:// doi.org/10.1016/0254-0584(84)90091-9.

27) K. Mosnackova, M. Mrlik, M. Micusik, A. Kleinova, V. Sasinkova, A. Popelka, A. Opalkova Siskova, P. Kasak, C.L. Dworak, J. Mosnacek, Light-Responsive hybrids based on carbon nanotubes with covalently attached PHEMA- g-PCL brushes, Macromolecules 54 (2021) 2412-2426, https://doi.org/10.1021/acs. macromol.0c02701.

Published in : Polymer (2023), vol. 278, article n°125992
DOI: 10.1016/j.polymer.2023.125992
Status : Postprint (Author's version)

28) M.E. Pekdemir, M. Koök, I.N. Qader, Y. Aydogdu, Preparation and physicochemical properties of mwcnt doped polyvinyl chloride/poly (e-caprolactone) blend, J. Polym. Res. 29 (2022) 1-9, https://doi.org/10.1007/s10965-022-02947-1.

29) B.P. Grady, Effects of carbon nanotubes on polymer physics, J. Polym. Sci. B Polym. Phys. 50 (2012) 591-623, https://doi.org/10.1002/polb.23052.

30) Wurm, D. Lellinger, A.A. Minakov, T. Skipa, P. Pöotschke, R. Nicula, I. Alig, C. Schick, Crystallization of poly(e-caprolactone)/MWCNT composites: a combined SAXS/WAXS, electrical and thermal conductivity study, Polymer 55 (2014) 2220-2232, https://doi.org/10.1016/j.polymer.2014.02.069.

31) T. Defize, R. Riva, J.M. Raquez, P. Dubois, C. Jerome, M. Alexandre, Thermoreversibly crosslinked poly(e-caprolactone) as recyclable shape-memory polymer network, Macromol. Rapid Commun. 32 (2011) 1264-1269, https://doi. org/10.1002/marc.201100250.

32) T. Chung, A. Romo-uribe, P.T. Mather, Two-Way Reversible Shape Memory in a Semicrystalline Network, 2008, pp. 184-192.

33) G. Floudas, L. Hilliou, D. Lellinger, I. Alig, Shear-Induced Crystallization of Poly (-caprolactone). 2, Evolution of Birefringence and Dichroism, 2000, pp. 6466-6472.

34) Gandini, The furan/maleimide Diels-Alder reaction: a versatile click-unclick tool in macromolecular synthesis, Prog. Polym. Sci. 38 (2013) 1-29, https://doi.org/ 10.1016/j.progpolymsci.2012.04.002.

35) C.-M. Chang, Y.-L. Liu, Functionalization of multi-walled carbon nanotubes with furan and maleimide compounds through Diels-Alder cycloaddition, Carbon N Y 47 (2009) 3041-3049, https://doi.org/10.1016/j.carbon.2009.06.058.

36) Xu, Z. Wang, Role of multi-wall carbon nanotube network in composites to crystallization of isotactic polypropylene matrix, Polymer 49 (2008) 330-338, https://doi.org/10.1016/j.polymer.2007.11.041.

37) K. Prashantha, J. Soulestin, M.F. Lacrampe, P. Krawczak, G. Dupin, M. Claes, Masterbatch-based multi-walled carbon nanotube filled polypropylene nanocomposites: assessment of rheological and mechanical properties, Compos. Sci. Technol. 69 (2009) 1756-1763, https://doi.org/10.1016/j.compscitech.2008.10.005.

38) A.K. Kota, B.H. Cipriano, M.K. Duesterberg, A.L. Gershon, D. Powell, S. R. Raghavan, H.A. Bruck, Electrical and rheological percolation in polystyrene/ MWCNT nanocomposites, Macromolecules 40 (2007) 7400-7406, https://doi.org/ 10.1021/ma0711792.

39) M. Landa, J. Canales, M. Fernandez, M.E. Munoz, A. Santamaría, Effect of MWCNTs and graphene on the crystallization of polyurethane based nanocomposites, analyzed via calorimetry, rheology and AFM microscopy, Polym. Test. 35 (2014) 101-108, https://doi.org/10.1016/j.polymertesting.2014.03.008.

40) K. Menzer, B. Krause, R. Boldt, B. Kretzschmar, R. Weidisch, P. Poötschke, Percolation behaviour of multiwalled carbon nanotubes of altered length and primary agglomerate morphology in melt mixed isotactic polypropylene-based composites, Compos. Sci. Technol. 71 (2011) 1936-1943, https://doi.org/ 10.1016/j.compscitech.2011.09.009.

41) D. Ren, Y. Chen, H. Li, H.U. Rehman, Y. Cai, H. Liu, High-efficiency dual- responsive shape memory assisted self-healing of carbon nanotubes enhanced polycaprolactone/thermoplastic polyurethane

Published in : Polymer (2023), vol. 278, article n°125992
DOI: 10.1016/j.polymer.2023.125992
Status : Postprint (Author's version)

composites, Colloids Surf. A Physicochem. Eng. Asp. 580 (2019), 123731, https://doi.org/10.1016/j.colsurfa.2019.123731.

42) J. Orellana, I. Moreno-villoslada, R.K. Bose, F. Picchioni, M.E. Flores, R. Araya- hermosilla, Self-healing polymer nanocomposite materials by joule effect, Polymers 13 (2021) 1-24, https://doi.org/10.3390/polym13040649